The effect of substrate temperature on the microstructure and tunnelling magnetoresistance of FeCo–Al_2O_3 nanogranular films

CHANGZHENG WANG*, XIAOGUANG XIAO
Department of Physics, Liaocheng University, Liaocheng City, Shandong Province 252000, People's Rebublic of China
E-mail: wcz102@sjtu.org

YONGHUA RONG, T. Y. HSU (XU ZUYAO)
School of Materials Science and Engineering, Shanghai Jiaotong University, Shanghai 200030, People's Rebublic of China

Published online: 12 April 2006

A series of FeCo–Al_2O_3 granular films were prepared with a magnetron controlled sputtering system. The magnetic–transport properties and microstructure of films sputtered at various substrate temperatures were characterized by conventional four probes method, SQUID magnetometer, analytical electron microscope and transmission electron microscope, respectively. The results indicate that the tunnelling magnetoresistance reaches the peak value of about 6.9% for FeCo (41 vol.%)-Al_2O_3 granular films sputtered at 300 K, while for FeCo granular films sputtered at 473 K, the 6% peak value in tunnelling magnetoresistance vs. volume fraction curve displaces toward the lower FeCo content of about 35 vol.%. Meanwhile, FeCo (30vol.%)-Al_2O_3 granular films sputtered both at room temperature and at 473 K behave as superparamagnetic and the susceptibility of this film increases with increasing substrate temperature. Based on the feature of microstructure of FeCo (41vol.%)-Al_2O_3 granular films sputtered at both room temperature and 823 K, the evolution sequence of two-stage phase separation is suggested. In addition, the effect of the microstructure on tunnelling magnetoresistance has been discussed.

1. Introduction

Since the discovery of the giant magnetoresistance (GMR) in granular films [1, 2], this phenomenon has been studied extensively because it provides a new perspective in the information industry and enriches the mechanism of GMR [3–6]. The granular films can be divided into two categories: ferromagnetic metal-metal granular films (FM-M) and ferromagnetic metal-insulator granular films (FM-I). Being slightly different from the FM-M granular films and similar to the ferromagnetic tunnelling junction [7, 8], the mechanisms of GMR in FM-I granular films is believed to be the spin-dependent tunneling, that is to say, the electron transport in FM-I films can be realized by intergranular tunnelling or temperature activated hopping when the volume fraction of magnetic granules is below the percolation threshold [9]. Therefore, in this case GMR can be called tunnelling magnetoresistance (TMR). It were discovered by Gitleman et al. [10] more then 30 years ago in discontinuous nickel films and discussed by Helman and Abeles [11].

A large magnetoresistive response in a low magnetic field is necessary for the materials that are used for magnetic sensors, etc. However, the saturation field of TMR for FM-I films is relatively high, as a result, it is difficult to use these films as magnetic sensors. As is well known, the TMR of nano-granular film is closely related to the film's structure such as the diameter of magnetic granules and the thickness of the oxide barriers [12]. Therefore, the TMR and its field response in a low magnetic field might be improved by controlling the film's structure by the deposition condition, such as substrate temperature and so on. In this paper, we will investigate the effect of substrate temperature on the magnetic–transport properties and microstructure of FeCo–Al_2O_3 nanogranular films.

*Author to whom all correspondence should be addressed.
0022-2461
DOI: 10.1007/s10853-006-6683-8

2. Experimental procedure

FeCo–Al_2O_3 granular films were sputtered respectively on KCl and glass substrate at various substrate temperatures with a spc350 multi-target magnetron controlled sputtering system. The base pressure was less than 3×10^{-3} Pa and the sputtering gas (Ar) pressure was 4×10^{-1} Pa. FeCo target (the weight ratio of Fe and Co is 1:1) and Al_2O_3 target (99.9% purity) were separately installed on two independently controlled R.F. cathodes, and were alternatively employed to sputter these films with substrate at a velocity of 30 circles per minute. The thickness of films is measured by α-step meter. For the samples with TEM observation, the thickness of films is about 50 nm, while the samples for TMR or SQUID measurement is about 300 nm. The volume fraction of FeCo in the FeCo–Al_2O_3 films was controlled by changing the sputtering power of FeCo target and was determined by means of energy dispersive spectrum (EDS) in JEM-2010 transmission electron microscope (TEM). TEM observations were carried out on JEM-100CX, JEM-2010 and Philips Tecnai F20 with electron energy-loss spectrometer (EELS) respectively. The magnetic properties were measured by a SQUID magnetometer and the applied field is from –5.5 T to 5.5 T.The TMR effect was measured by a conventional four-probe method and the applied field is from –1.3 T to 1.3 T.

3. Results and discussion

3.1. Microstructure

Fig. 1 shows a representative of the HRTEM micrograph and its corresponding Fourier transformed pattern inserted in the right lower corner for a FeCo (41 vol.%)-Al_2O_3 film. The film was prepared on the substrate at room temperature (RT, about 300 K). As seen in Fig. 1, the structure of the film consists of the FeCo metallic granules with a diameter of about 2–4 nm and Al_2O_3 insulating narrow boundaries with the width of about 1–2 nm. No lattice fringes in HRTEM image and its corresponding spots in Fourier transformed pattern can be observed in Fig. 1, indicating these particles are amorphous phase or cluster.

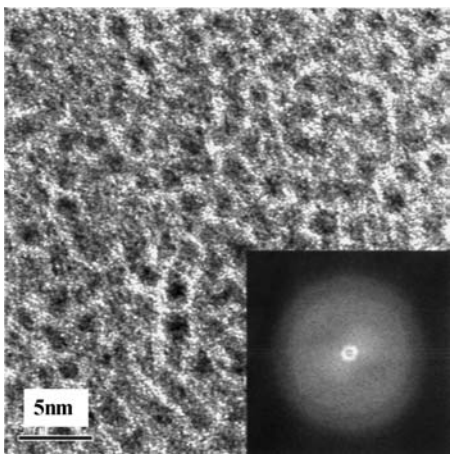

Figure 1 HRTEM image of FeCo(41 vol.%)-Al_2O_3 film sputtered at RT and its corresponding Fourier transformed pattern.

Fig. 2 (a) is the TEM bright field image of FeCo(41 vol.%)-Al_2O_3 granular film sputtered at RT. It can be found that a little amount of α-Fe (Co) particles with bcc structure (see Fig. 2(b)) disperse in amorphous Al_2O_3 matrix. EDS analysis as shown in Fig. 2 (c) reveals that all particles contain both Fe and Co atoms. The above experiments indicate that FeCo(41 vol%)-Al_2O_3 films sputtered at room temperature consist of mostly amorphous FeCo granules in amorphous Al_2O_3 matrix with a small amount of FeCo granules being alpha-Fe(Co) with a bcc structure.

With increasing substrate temperature, the structure of film has been changed. Fig. 3 (a) and (b) show the TEM bright field image of FeCo(41 vol.%)-Al_2O_3 granular film sputtered at 473 K and 823 K. As can be seen that the granule size increases with increasing substrate temperature. This change also can be confirmed by XRD spectrum. Fig. 4 shows the XRD spectrum of FeCo(41 vol.%)-Al_2O_3 granular film sputtered at RT and 473 K, respectively. It was clear that a broad diffraction peak occurred in the vicinity of 44°, indicating that all granules in film are either amorphous or smaller granules with bcc structure. With increasing substrate temperature, the strength of broad diffraction peak increases and the width of broad diffraction peak decreases, implying that the granule size increases.

Fig. 5 shows HRTEM images and their selected area diffraction pattern (SADP) of Fe and Co particles in 823 K sputtered FeCo(41 vol.%)-Al_2O_3 film. HRTEM imaging of Co (Fig. 5(a)) and Fe (Fig. 5(b)) particles was carried out after they were identified by their EELS maps respectively, and show the lattice fringes or two- dimensional structures of Co particles and Fe as the crystalline feature, meanwhile, also show the crystalline and amorphous feature of Al_2O_3 or ferrous oxide.

Comparing with Fig. 5(a) and 5(b) it can be found that the interface between Co and Al_2O_3 is sharper than that between Fe and Al_2O_3, which may be explained as the existence of oxygen in Fe particles. In addition, Fig. 5(c) shows that diffraction rings accompanying with brighter diffraction spots in selected area diffraction pattern (SADP) for 823 K sputtered film is sharper than those for as-RT sputtered film, which indicates the existence of the crystalline bcc Fe (α-Fe) and hcp Co(α-Co) particles as indexed in Fig. 5(c) for 823 K sputtered film.

By the comprehensive analysis of RT sputtered and 823 K sputtered films, the evolution sequence of the two-stage phase separations for the FeCo–Al_2O_3 granular film is suggested as follows. If the RT sputtered FeCo–Al_2O_3 film is gradually heated up below 823 K, the amorphous phase or cluster containing both Fe and Co atoms will firstly transform to the super-saturation bcc α-Fe(Co) particles by crystallization, promoting the phase separation between α-Fe (Co) and Al_2O_3, then the super-saturation α-Fe (Co) gradually precipitates α-Co particles to further produce the phase separation between Fe and Co until

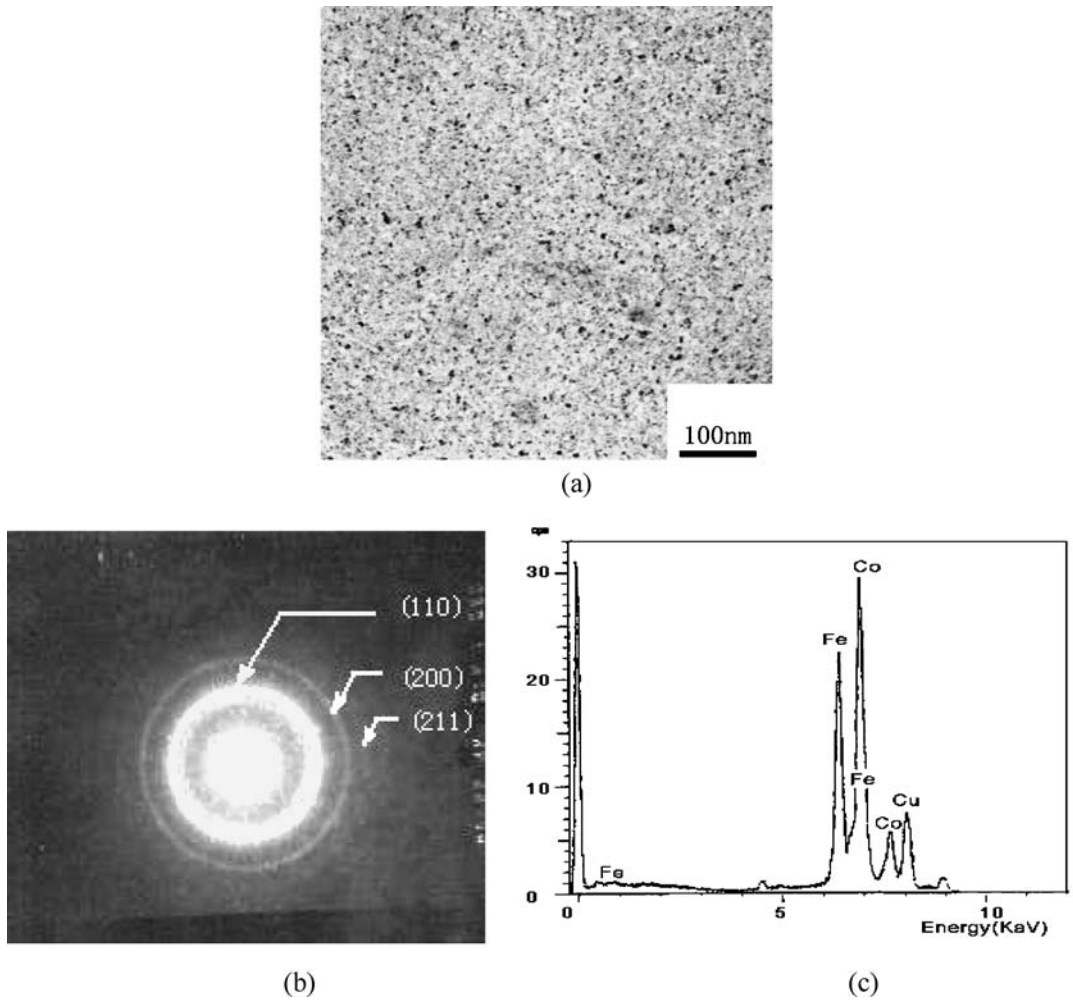

Figure 2 Analysis of particles in FeCo(41 vol.%)-Al_2O_3 film sputtered at RT, (a) Bright field image, (b) Selected area diffraction pattern, (c) EDS of a particle (Cu peak from copper grid).

to the equilibrium state. It is conceivable that the proper annealing technology resulting in the phase separation is favorable for the improvement of GMR effect for RT sputtered FeCo–Al_2O_3 granular films.

3.2. Magnetic–transport properties

It is well known that inherent to FM-I granular films is the phenomenon of percolation and hence there exist a percolation threshold x_c that is about 0.5–0.6 [13]. When

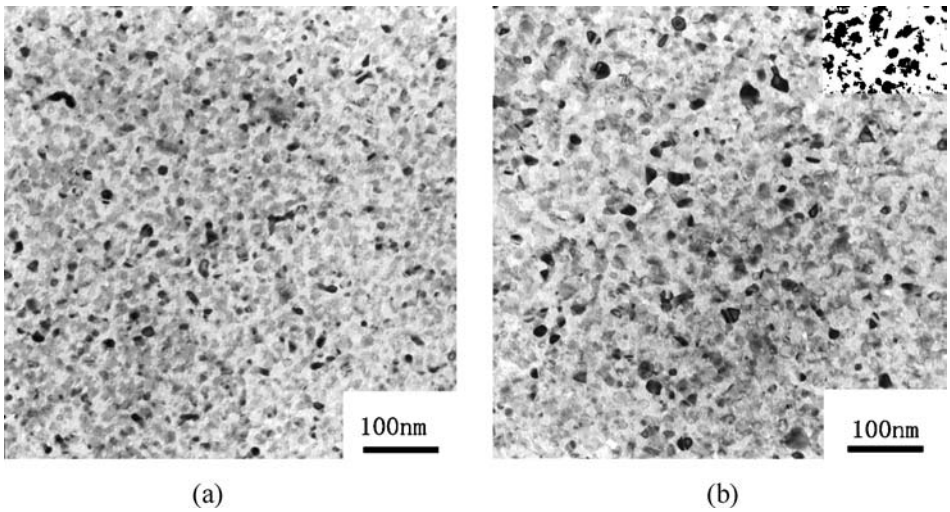

Figure 3 TEM bright field image of FeCo(41 vol.%)-Al_2O_3 granular film (a) sputtered at 473 K, (b) sputtered at 823 K.

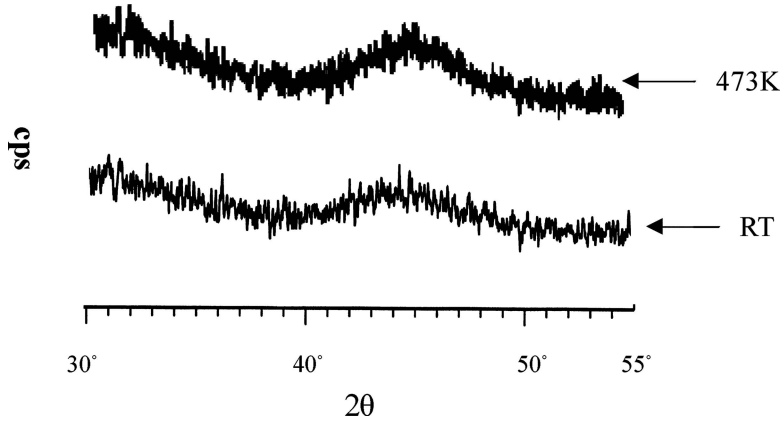

Figure 4 XRD spectrum of FeCo(41 vol.%)-Al_2O_3 granular film sputtered at RT and 473 K.

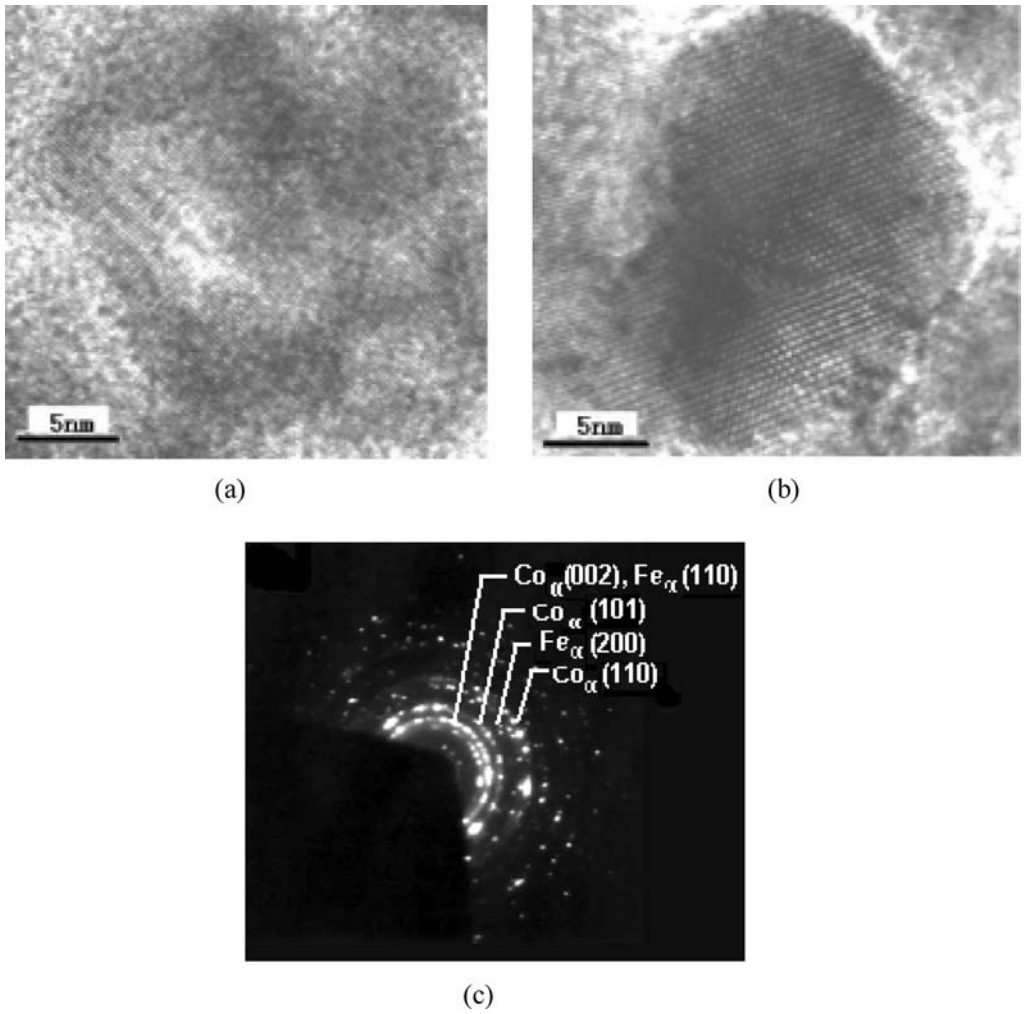

Figure 5 HRTEM images and their SADP of Fe and Co particles in 823 K sputtered FeCo(41 vol.%)-Al_2O_3 film. (a) Fe particles, (b) Co particles, (c) SADP.

the volume fraction is larger than x_c, small granules can aggregate into a connecting network, leading to the fact that the granular films have metallic conductivity. While when the volume fraction is less than x_c, the granular films can exhibit insulator-like conductivity since magnetic granules are few and separated by the insulator host. That is to say that the conductance in FM-I granular films can be divided into three regions with metallic, intermediate and insulator-like conductivity. The measured room temperature resistivities of granular films sputtered both at 300 K and at 473 K also exhibit such behaviour, as shown in Fig. 6. It is clear that the resistivity of granular films sputtered both at 300 K and at 473 K decreases with increasing the FeCo volume-fraction. By varying the

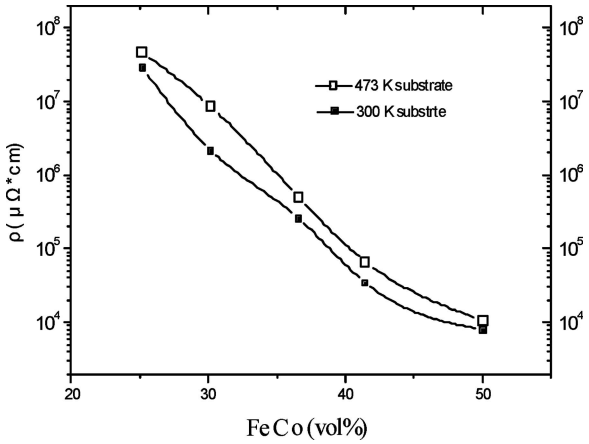

Figure 6 Curve of TMR vs. FeCo volume-fraction.

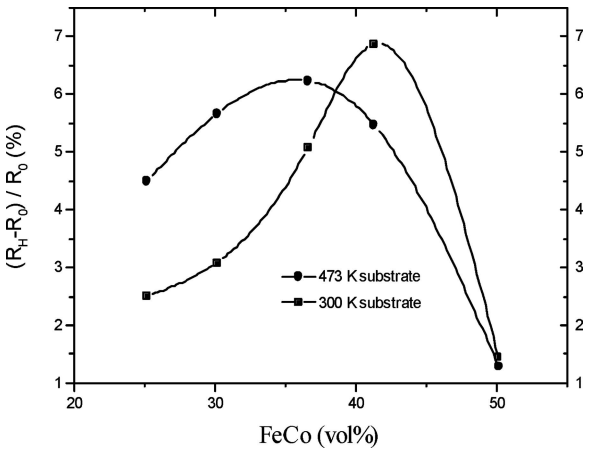

Figure 7 Curve of TMR vs. FeCo volume-fraction.

volume fraction, the resistivity can be changed over three orders of magnitude and don't alter apparently in the volume fraction from about 25% to about 50%, indicating that the conducting mechanism of electrons don t change and only behaves as insulator-like in this region where the volume fraction is less than x_c. On the other hand, it can be seen that the higher the substrate temperature, the higher the resistivity, which is attributed to the fact that with increasing substrate temperature, both the granule size and the thickness of tunnelling barrier increase, thus leading to the reduction of tunnelling probability of the conducting electrons and then the increase of resistivity [11].

To investigate further the mechanism of magnetic-transport of the films, we have discussed the effect of the substrate temperature on the TMR effect. Fig. 7 shows the dependence of TMR on the FeCo volume-fraction in granular films sputtered at 300 K and 473 K, respectively. As can be seen that for the granular films sputtered both at 300 K and at 473 K, the TMR effects increase initially with increasing the volume-fraction, reaching the peak value of about 6.9% for FeCo–Al_2O_3 granular films sputtered at 300 K and the peak value of 6% for FeCo–Al_2O_3 granular films sputtered on 473 K, and beyond the peak value, both TMR effects decrease with increasing the FeCo volume-fraction, reaching a zero value simultaneously at about 52 vol.% FeCo that is in the range of percolation threshold, x_c [13]. Meanwhile, the peak in GMR vs. volume-fraction curve displaces from about 41 vol.% FeCo to the low content about 35 vol.% FeCo when the substrate temperature ranges from 300 K to 473 K, leading to a overlap in the curves of TMR vs. FeCo volume-fraction at a certain FeCo volume-fraction, below which the GMR value increases with increasing the substrate temperature, while above which the MR value decreases with increasing the substrate temperature.

As mentioned above, the large TMR appears only in the samples with FeCo volume-fraction less than x_c. If FeCo volume-fraction is larger than x_c, all the FeCo granules coalesce and gradually form a connecting network structure. The electric transport in this region is not realized by tunnelling but carried by metallic conductance. Also, the mean free path of electrons becomes smaller than the granule size and thus the electron spins must interact with a varying magnetization distribution. Consequently, TMR vanishes. However, in the region where FeCo volume-fraction is smaller than x_c, the TMR increases with decreasing FeCo volume-fraction, reaching a maximum in a middle region. As FeCo volume-fraction decreases

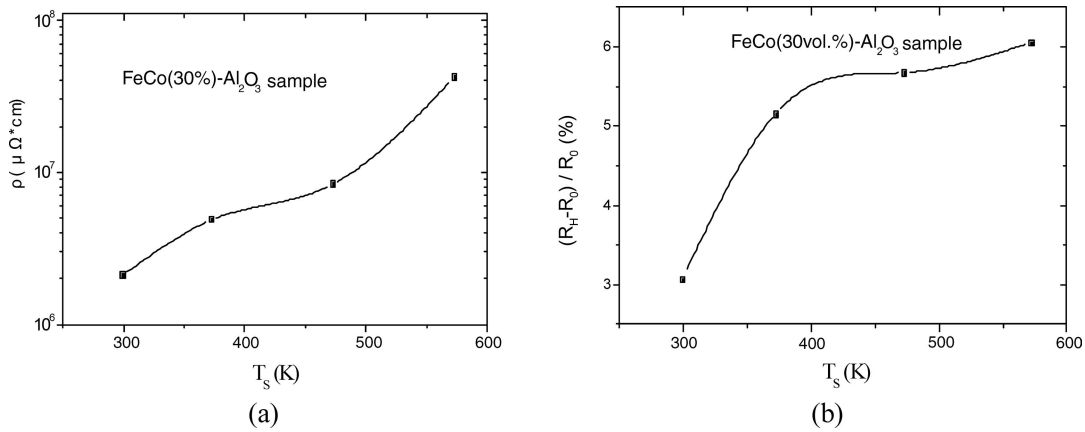

Figure 8 (a) Resistivity and (b) GMR dependence of substrate temperature for FeCo(30 vol%.)-Al_2O_3 samples, respectively.

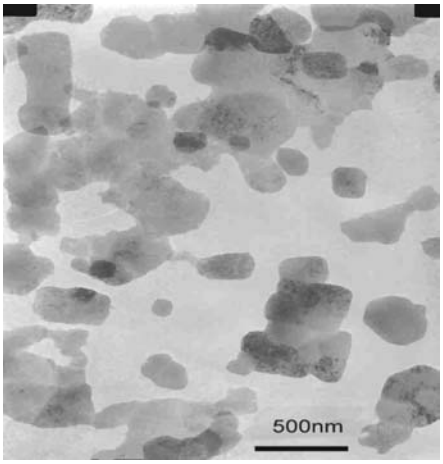

Figure 9 TEM micrograph of FeCo 41 vol.%-Al_2O_3 films with substrate temperature at 823 K.

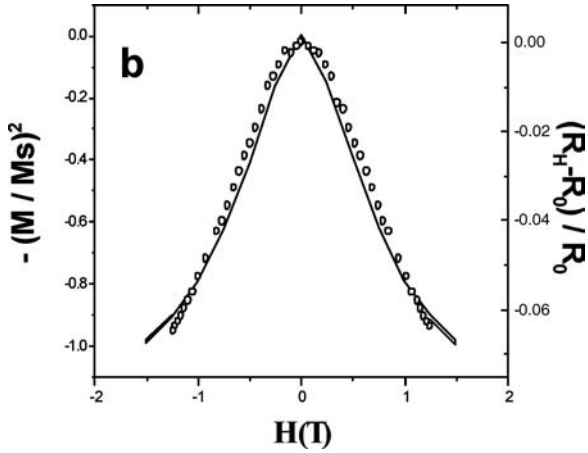

Figure 10 The fitting of TMR vs. $-(M/M_S)^2$.

further, the TMR drops. In this region the electric transport is governed by tunnelling current between FeCo granules separated by Al_2O_3 tunnel barriers. The thickness of tunnelling barriers is a crucial factor for resistivity and TMR in granular films [14, 15]. Fig. 8 (a) shows the dependence of the resistivity of FeCo(30 vol.%)-Al_2O_3 granular films on the substrate temperature. It is clear that the resistivity of FeCo(30 vol.%)-Al_2O_3 granular films increases with increasing substrate temperature. This is attributed to the fact that the higher the substrate temperature, the larger the thickness of tunnelling barrier between neighbour FeCo granules, and hence leading to the higher resistivity [11]. In addition, the thickness of tunnelling barriers exists a critical value L_c having a close relationship with the spin diffusion length [14], above which the TMR value reduces due to the spin-flip tunnelling, while below which the TMR value increases monotonically with increasing the thickness of tunnel barrier, i.e., the wider the tunnel barrier, the larger the TMR ratio. These phenomenons can be illustrated in our experiments.

According to the effect of the substrate temperature on the TMR (see Fig. 7), we can divide the granular films with the volume fraction less than x_c into two categories. One is the granular films whose volume fraction is far from x_c such as FeCo(30 vol.%)-Al_2O_3 granular films. In these granular films, the TMR value increase with increasing the substrate temperature (see Fig. 7 and Fig. 8 (b)), i.e. the TMR value increases with increasing the thickness of tunnelling barrier. This implies that that the thickness of tunnel barrier of this granular film is smaller than the critical value. The other is the granular films with higher FeCo volume-fraction, such as FeCo(41 vol.%)-Al_2O_3 granular film. The TMR value of this film decreases with increasing the substrate temperature (as shown in Fig. 7), which arises from the fact that on one hand, the granules can coalesce easily and then form multidomain structure that diminishes the TMR value [16] with increasing substrate temperature; on the other hand, the granules can also form easily the network in films with higher FeCo volume-fraction. Further confirmation came from the TEM micrographs. Fig. 9 shows the micrograph of FeCo (41 vol.%)-Al_2O_3 films with substrate temperature at 823 K. It is clear that the granules can conjugate and form network, thus leading to the drop of TMR. For FeCo(30 vol.%)-Al_2O_3 granular films, the thickness of tunnelling barrier may be less than the critical value L_c when substrate temperature is below 573 K, as a result, the TMR effect increase with increasing substrate temperature (see Fig. 8 (b)). However, it is conceivable that the TMR effect in this films maybe diminishes with further increasing substrate temperature due to the fact that the granules can form multidomain structure and the thickness of tunnelling barrier can be larger than the critical value L_c.

In granular films, the GMR effect has something to do with the magnetic property. Zhang et al. [17] obtained the following formulas between the GMR effect and magnetisation M, if all of the granules behave superparamagnetic and have equal size.

$$GMR = \frac{R(H) - R(0)}{R(0)} = -A\left(\frac{M}{M_S}\right)^2 \qquad (1)$$

where A is a constant that bears a closely relationship to the granule size and the volume-fraction of magnetic granules and can be expressed as follows [18].

$$A = \frac{\rho_m}{\rho_m + \rho_{ph} + \rho_0} \qquad (2)$$

where ρ_m is magnetic resistivity, ρ_{ph} phonon resistivity, and ρ_0 residual resistivity.

To identify the relationship between the GMR effect and magnetization, we carried out a fitting using Eq. (1), as shown in Fig. 10. Here, the circles and the solid line represent the measured magnetoresistance value and the value $-(M/Ms)^2$, respectively. It can be seen that the fitting between the measured MR value and the calculated value is very good except that there exists a deviation in the high field, which is in agreement with the experiments

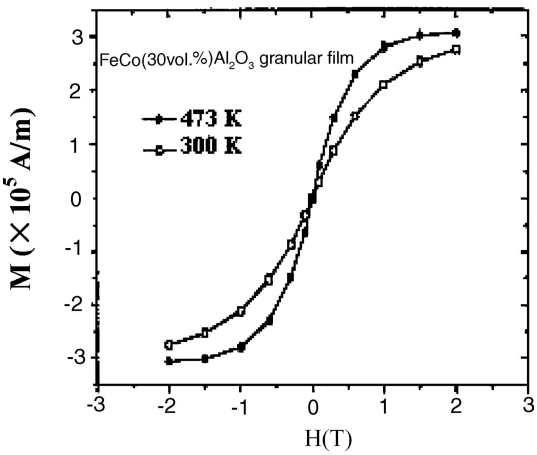

Figure 11 The curve of M-H at various substrate temperatures for FeCo(30 vol%.)-Al_2O_3 films.

of Xiao's [2]. However, Gregg [19] found it fit well in high field, while in low field, the linear relationship between GMR and $(M/Ms)^2$ was severely deviated.

In addition, the effect of substrate temperature on the magnetic properties also has been studied. Fig. 11 shows the M-H curve of FeCo 30% vol.-Al_2O_3 films with substrate temperature at RT and at 473 K. As can be seen that the granular films sputtered both at RT and at 473 K are superparamagnetic and the susceptibility increases with increasing substrate temperature, which is attributed to the fact that with increasing substrate temperature granules can grow to be a larger one which is easier to saturate than smaller one under applied fields.

4. Conclusions

(a) The TMR of FeCo–Al_2O_3 film sputtered at RT reaches the peak value of about 6.9% in the vicinity of about 41 vol.% FeCo, while for FeCo–Al_2O_3 granular films sputtered at 473 K, the 6% peak value in TMR vs. volume fraction curve displaces toward the lower content about 35 vol.% FeCo.

(b) The resistivities increase with increasing substrate temperature, indicating that the higher the substrate temperature, the larger the thickness of tunnel barrier, and thus the higher the resistivities. While for TMR effect, it increases with increasing substrate temperature in granular films with low FeCo volume-fraction and decreases with increasing substrate temperature in granular films with high FeCo volume-fraction. Meanwhile, the susceptibility of FeCo (30 vol.%)-Al_2O_3 granular films increases with increasing substrate temperature.

(c) The evolution sequence of two-stage the phase separations of FeCo (41 vol.%)-Al_2O_3 film is suggested, namely, the super-saturation α-Fe (Co) particles firstly form through amorphous crystallization, promoting the first phase separation between α-Fe (Co) and Al_2O_3, then the hcp α-Co particles appear through the precipitation of Co atoms from the super-saturation α-Fe (Co), which leads to the second phase separation between Fe and Co.

Acknowledgements

The present work is financially supported by the National Nature Science Foundation of China under Grant No.50071033 and Hi-Tech Research and development Program of China under Grant No.2004AA32G090.

References

1. A. E. BERKOWITZ, J. R. MITEKELL and M. J. COREY, et al., *Phys. Rev. Lett.* **68** (1992) 3745.
2. J. Q. XIAO, J. S. JIANG and C. L. CHIEN, *ibid.* **68** (1992) 3749.
3. N. PELEG, S. SHTRIKMAN and G. GORODETSKY, et al., *J. Magnet. Mag. Mater.* **191** (1999) 349.
4. YAN JU, CHEN X U. and ZHEN-YA LI, *J. Magnet. Mag. Mater.* **233** (2001) 267.
5. A. MILNER, I. YA KORENBLIT and A. GERBER, *Phys. Rev. B* **60** (1999) 14821.
6. G. J. STRIJKERS, H. J. M. SWAGTEN and B. RULKENS et al., *J. Appl. Phys.* **84** (1998) 2749.
7. J. C. SLONCZEWSKI, *Phys. Rev. B* **39** (1989) 6995.
8. S. MAEKAWA and U. GÄFVERT, *IEEE Trans. Mag.* **18** (1982) 707.
9. A. MILNER, A. GERBER and B. GROISMAN, et al., *Phys. Rev. Let.* **76** (1996) 475.
10. J. I. GITTLEMAN, Y. GOLDSTEIN and S. BOZOWSKI, *Phys. Rew. B* **5** (1972) 3609.
11. J. S. HELMAN and B. ABELES, *Phys. Rew. Lett.* **37** (1976) 1429.
12. M. OHNUMA, K. HONO and E. ABE, et al., *J. Appl. Phys.* **82** (1997) 5646.
13. C. L. CHIEN, *J. Appl. Phys.* **69** (1991) 5267.
14. W. YANG, Z. S. JIANG and Y. W. DU, et al., *Solid State Communi.* **104** (1997) 479.
15. J. S. HELMAN and B. ABELES. *Phys. Rev. Let.* **37** (1976) 1429.
16. A. HÜTTEN, J. BERNARDI and C. NELSON, et al., *Phys. Status. Solidi* (a) **150** (1995) 171.
17. S. ZHANG and P. M. LEVY, *J. Appl. Phys.* **73** (1993) 5315.
18. C. L. CHIEN, J. Q. XIAO and J. S. JIANG, *J. Appl. Phys.* **73** (1993) 5309.
19. J. F. GREGG, S. M. THOMPSON and S. J. DAWSON, et al., *Phys. Rev. B* **49** (1994) 1064.

Received 17 June
and accepted 29 August 2005